EFFECT OF MELAMINE ACIDIC TREATMENT ON g-C_3N_4 PHYSICOCHEMICAL PROPERTIES AND CATALYTIC ACTIVITY

[1*]*Andrei Ivanets, Vladimir Prozorovich*

[1]Institute of General and Inorganic Chemistry of the National Academy of Sciences of Belarus, Minsk, 220072, Belarus.

[*]Corresponding author: ivanets@igic.bas-net.by

Abstract

Heterogeneous photocatalysts are widely used for wastewater and natural water treatment from organic pollutants. In this paper, g-C_3N_4-based photocatalysts were synthesized by thermal condensation of melamine. The effect of melamine pretreatment with acetic acid on the physicochemical properties of g-C_3N_4 was studied using differential thermogravimetric analysis (DTA-TG), X-ray diffraction (XRD), FT-IR spectroscopy, scanning electron microscopy (SEM), and low-temperature nitrogen adsorption-desorption. The catalytic activity of synthesized photocatalysts was evaluated during the oxidative degradation of Rhodamine B in an aqueous solution under “soft” (type A) and “hard” (type B) UV irradiation.

Key words: g-C_3N_4; Synthesis; Advanced Oxidation Process; Photocatalyst; Rhodamine B; Wastewater Treatment

Introduction

Heterogeneous catalytic processes are widely used for water purification from toxic organic pollutants (Zhang 2020). Organic dyes, pharmaceutically active compounds, trihalolmethanes and pesticides are among the most common toxic impurities that pose a significant risk to human health and the environment (Lu 2020). Fenton-like catalysts based on iron oxides (Thomas 2021), metal ferrites (Ivanets 2020), double layered metal hydroxides (Valeikiene 2020; Zhao 2020), as well as photocatalysts based on TiO_2 (Chen 2020) and a number of other semiconductor materials (ZnO, WO_x, SnO_2, CdS, etc.) are widely studied as promising materials for the oxidative degradation of the above pollutants (Zhu 2019).

Graphitic carbon nitride (g-C_3N_4) attracts special attention as a heterogeneous photocatalyst due to its high chemical and thermal stability and electronic structure (Yang 2020; He 2020). Carbon nitride is an organic polymer semiconductor and exists in five different allotropic forms: α-C_3N_4,

β-C_3N_4, g-C_3N_4, cubic and pseudocubic modifications. g-C_3N_4 is one of the most stable allotropic modifications with a complex two-dimensional graphite-like planar structure, where N-heteroatoms are substituted in a graphite framework containing π-conjugated systems, with a distance between the two layers of 0.326 nm (Dong 2014).

In the last decade, various methods for carbon nitride producing have been developed, including chemical vapor deposition, polymerization, thermal condensation, solvothermal, sonochemical and hydrothermal synthesis. g-C_3N_4 is usually prepared using thermal condensation, forming a conjugated aromatic heptazine graphite-like structure. The most commonly used organic nitrogen-containing precursors are cyanamide, dicyandiamide, melamine, triazine, heptazine derivatives and urea and thiourea. During heat treatment, condensation of C-N bonds occurs, which leads to the formation of two-dimensional tri-S-triazine sheets bound via tertiary amino groups.

The physicochemical and catalytic properties of g-C_3N_4 significantly depend on the precursor nature and the thermal condensation conditions. Preliminary conversion of melamine to the salt form allows controlling the polymerization and condensation processes, and as a result, to vary the chemical structure, texturing characteristics, size and morphology of g-C_3N_4 particles.

In this work, mesoporous g-C_3N_4 samples were synthesized by thermal condensation using melamine and its acetate form as a precursor, their physicochemical properties were studied, and the photocatalytic activity in the Rhodamine B dye oxidative degradation reaction was evaluated.

Materials and Methods

Synthesis of g-C_3N_4

g-C_3N_4 samples were synthesized by thermal condensation of melamine $C_3H_6N_6$ (99.9%, Five oceans Ltd., Belarus) or its acetate form. Carbon nitride samples obtained from melamine and its acetate form were labeled as g-C_3N_4 and g-C_3N_4-acetate, respectively. To prepare the acetate form, 1.0 g of melamine was mixed with 23.7 mL of 1.0 M acetic acid CH_3COOH (99.9%, Five oceans Ltd., Belarus), which corresponds to the equimolar amount of $–NH_2$ and –COOH groups. Then the resulting suspension was kept under constant stirring on a magnetic stirrer at 65 °C for 1.5 hours until the mixture was completely evaporated. A sample of 10.0 g of melamine or its acetate form was placed in a corundum crucible and calcined in a laboratory furnace SNOL 6.8/1300 at 550 °C for 2 hours at a heating rate of 2.5 °C/min. During the heating process, melamine was first formed by melem (white powder), which, during subsequent polymerization, turned into g-C_3N_4. The resulting yellow powders were crushed in an agate mortar for further study of physicochemical properties and evaluation of photocatalytic activity.

Methods of g-C_3N_4 characterization

Differential thermogravimetric analysis (DTA-TG) was performed using a Paulik-Paulik-Erdei derivatograph (Hungary) by melamine samples heating in the air atmosphere in the temperature range of 20-600 °C at a heating rate of 2.5 °C/min. The weight of the analyzed samples was 200 mg. X-ray diffraction analysis was performed on the ADVANCED D8 Bruker diffractometer (Germany) using CuK_α radiation. The FT-IR spectra of the samples were recorded on an IR spectrometer with a Fourier transform FTIR M2000 Midac (USA). The spectra were processed using the Grams 32 program from Galactic (USA). The spectra were recorded at room temperature by tableting with KBr in the range of 4000-450 cm^{-1}. Adsorption and texture characteristics were studied by low-temperature nitrogen adsorption-desorption on the surface and porosity analyzer ASAP 2020 Micromeritics (USA). The specific surface area was calculated using the single-point Brunauer-Emmett-Teller method (A_{BET}), the pore volume (V_{total}), the average pore diameter ($D_{BJH\ des}$), and the pore diameter distribution were calculated using the Barrett-Joyner-Halenda (BJH) method for desorption isotherm branch. The surface morphology of g-C_3N_4 samples was evaluated by electron microscopy using a JEOL-5610LS scanning electron microscope (Japan).

Photocatalytic experiment

An aqueous solution of 20.0 μm of Rhodamine B (99.8%, Five oceans Ltd., Belarus) was prepared without pH correction for evaluating of samples photocatalytic activity. 50.0 mg catalyst sample was placed in 50.0 mL of model solution and kept in the dark for 1 hour to reach of adsorption equilibrium. Further, the catalyst suspension was irradiated by “soft” and “hard” UV at a wavelength of 320-400 nm (type A) and 240-320 nm (type B) using a medium-pressure mercury quartz lamp (375 W, Russia). The concentration of the Rhodamine B dye was measured on a scanning spectrophotometer of the Metertech SP-8001 brand (Taiwan) at a wavelength of 554 nm. Calculations of obtained data was performed using first order kinetic equation in linear form:

$$\ln(C_0/C_t) = \ln C_e - k' t,$$

where C_t - equilibrium Rhodamin B concentration at time *t* (μM), C_0 – initial concentration (μM), k' - the apparent rate constant (min^{-1}), t – reaction time (min).

Results and discussion

From the data of differential thermal analysis (Fig. 1), it follows that the process of melamine condensation and deamination occurs in the range of 300-370 °C, which is confirmed by the corresponding endothermic effects with maxima at 340 and 330 °C, accompanied by mass losses of 65 and 70% for pure melamine and its acetate form, respectively. Further heating to 460-470 °C

DOI: https://doi.org/10.20535/wptstn.v28i3.216100

was accompanied by a slight loss of mass, which probably corresponds to the melem (2,5,8-triaminotri-s-triazine) formation and a slight sublimation of the obtaining products.

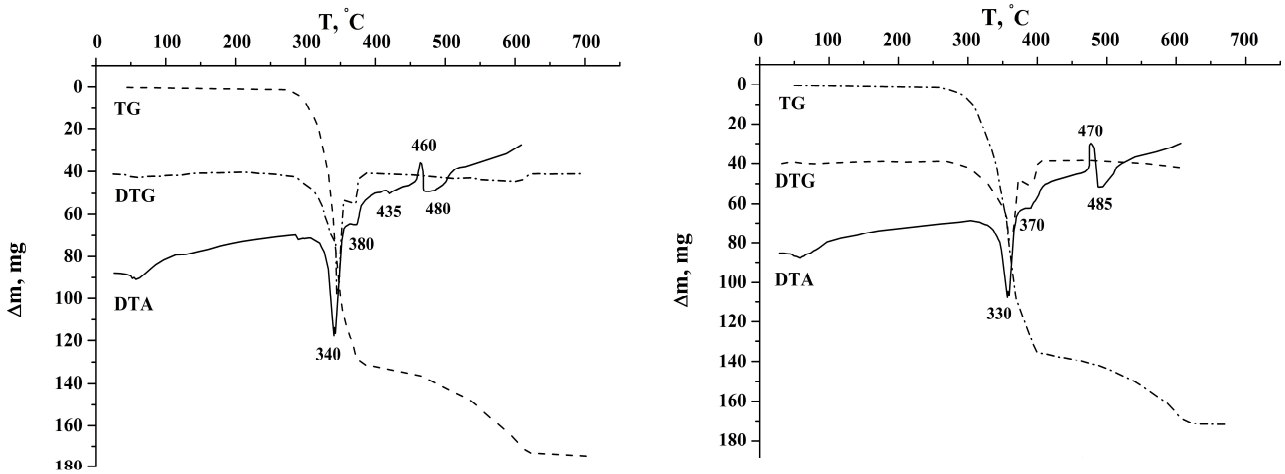

a b

Fig. 1. DTA-TG analysis of (a) g-C_3N_4 and (b) g-C_3N_4-acetate samples.

For both samples, the presence of an endothermic effect was observed with a maximum at 460 and 470 °C, which is usually attributed to the process of melem converting into graphitic carbon nitride. All thermal effects ended at 520-550 °C, which made it possible to choose the temperature for g-C_3N_4 synthesis.

XRD data of g-C_3N_4 samples (Fig. 2a) had two pronounced peaks at 27.35 and 27.38°, which correspond to (002) characteristic of interlayer reflection in the structure of graphitic carbon nitride (Zhang 2012). Less pronounced peaks at 13.11 and 12.84° refer to (001) and indicate in-plane structure (Zhang 2010).

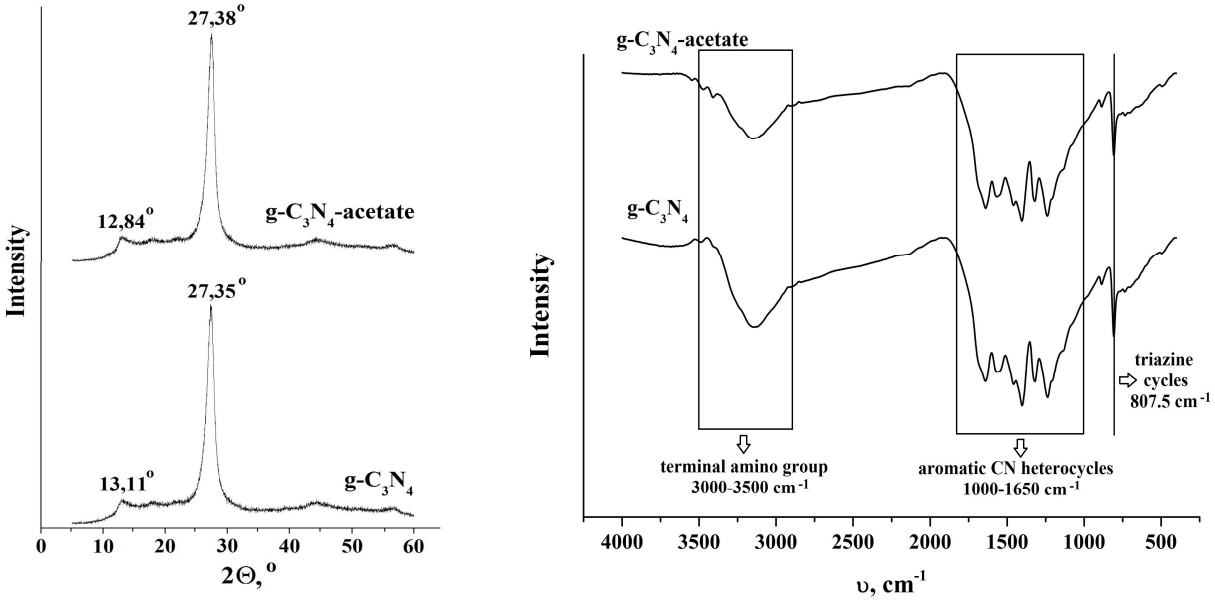

a b

Fig. 2. (a) XRD patterns and (b) FT-IR spectra of g-C_3N_4 and g-C_3N_4-acetate samples.

Thus, the synthesized samples were identified as g-C_3N_4 and had similar crystal structure without significant changes in the interlayer and in-plane structure. All detected XRD peaks for g-C_3N_4 samples obtained from melamine and its acetate form were in good agreement with previously reported data (Wu 2015).

IR spectroscopy data allow for more detailed identification of the chemical structure of the obtained samples (Fig. 2b). All spectra shown a sharp absorption peak at 807 cm^{-1}, corresponding to the valence vibrations of triazine rings. The peaks in the region of 1570-1634 and 1258-1480 cm^{-1} belong to the typical fluctuations of C=N-C bonds that are characteristic of the conjugated aromatic structure (Wang 2020). In addition, peaks at 1238, 1322, and 1402 cm^{-1} that correspond to the C-N bond in aromatic secondary and tertiary amines can be attributed to dimelem formation. All the absorption bands of the IR-spectra were quite intense, which indicates a high degree of condensation and was in good agreement with the XRD data (Fig. 2a). Consequently, the intensity of the absorption peaks seems to depend strongly on the degree of polycondensation of the tri-s-triazine system derivatives. Wide peaks between 2980 and 3340 cm^{-1} (M3) and at 3433 cm^{-1} can be attributed to fluctuations in the -NH/-NH_2 and -OH groups, respectively.

Low-temperature nitrogen adsorption-desorption isotherms (Fig. 3) belong to type IV according to the IUPAC classification (Thommes 2015), which is typical for mesoporous solids. The capillary-condensation hysteresis loop for both samples belonged to the H3 type and had a sharp increase in adsorption at relatively high values of P/P_0 ~0.90-0.95. This type of hysteresis loop is typical for adsorbents with slit-like pores formed when packing plane-parallel particles.

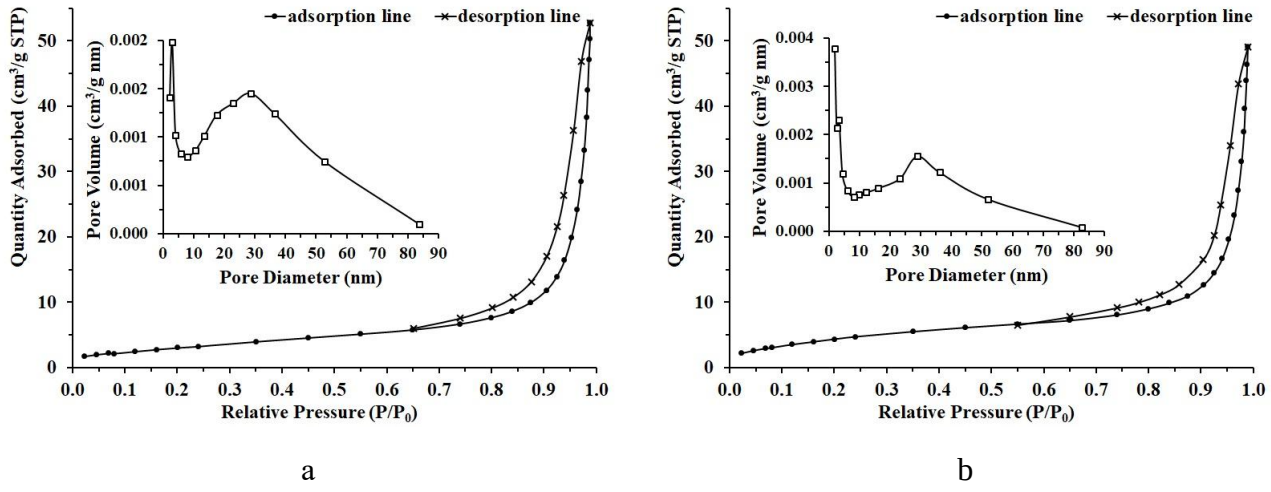

Fig. 3. Isotherms of low-temperature nitrogen adsorption-desorption and pore size distribution of (a) g-C_3N_4 and (b) g-C_3N_4-acetate samples.

The pore size distribution curves had a mostly blurred peak in a wide range from 10 to 80 nm, which indicates the heterogeneity of the porous structure and the polydisperse pore size distribution for g-C_3N_4 samples. The g-C_3N_4-acetate sample was characterized by a larger pore structure

($D_{des\ BJH}$ of 27.9 nm) compared to g-C_3N_4 ($D_{des.BJH}$ of 17.8 nm). This results in a significant reduction in the specific surface area of graphitic carbon nitride from 17.2 to 11.5 m^2/g in case of melamine and its acetate form as precursors. Regardless of the precursor nature, the obtained samples had a close pore volume of ~0.06 cm^3/g (Table 1).

Table 1. Adsorption characteristics of g-C_3N_4 samples.

Characteristic	g-C_3N_4	g-C_3N_4-acetate
Specific surface A_{BET}, m^2/g	17.2	11.5
Pore volume V_{total}, cm^3/g	0.061	0.066
Pore diameter $D_{des.}$, nm	17.8	27.9

The surface morphology of carbon nitride samples is shown in Fig. 4. SEM images clearly identify micron-sized lamellar agglomerates consisting of smaller needle-shaped particles. The presence of these particles was more typical for g-C_3N_4 sample (Fig. 4a). Scanning electron microscopy data were in good agreement with the results of low-temperature nitrogen adsorption-desorption.

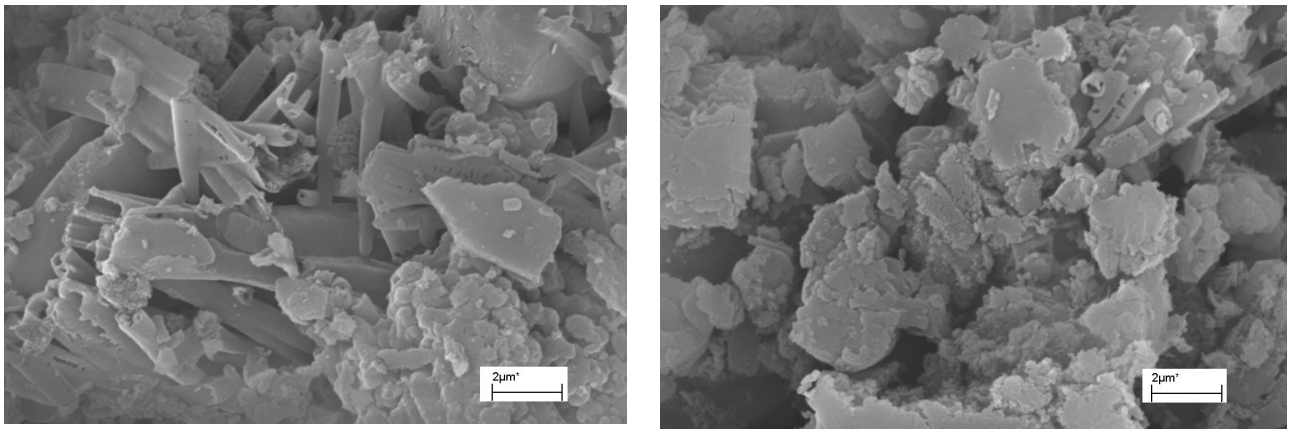

a b

Fig. 4. SEM images of surface (a) g-C_3N_4 and (b) g-C_3N_4-acetate samples (×15 000).

The results of photocatalytic Rhodamine B degradation on graphitic carbon nitride samples are shown in Fig. 5. The kinetics of catalytic dye degradation on g-C_3N_4 samples using "soft" (type A) and "hard" (type B) UV irradiation was reliably described by the first-order kinetics model. The g-C_3N_4-acetate sample had a higher catalytic activity compared to g-C_3N_4. Thus, during 150 min under “soft” UV irradiation (type A), the degree of Rhodamine B dye catalytic degradation was 0.7 (k' 0.006 min^{-1}) and 0.8 (k' 0.008 min^{-1}) for g-C_3N_4 and g-C_3N_4-acetate samples, respectively (Fig. 5a, 5c).

According to X-ray and IR-spectroscopy data, obtained graphitic carbon nitride samples had a very similar structure, so the differences in catalytic activity were probably due to their differences in porous structure. Despite the fact that the g-C_3N_4 sample had a higher specific surface area (A_{BET} of

DOI: https://doi.org/10.20535/wptstn.v28i3.216100

17.2 m^2/g) compared to g-C_3N_4-acetate (A_{BET} of 11.5 m^2/g), the g-C_3N_4-acetate sample was characterized by higher catalytic activity. This may be due to the larger-pore structure of the g-C_3N_4-acetate sample ($D_{des.BJH}$ of 27.9 nm), which contributes to the adsorption of Rhodamine B molecules and caused the availability of catalytic centers on surface catalyst for dye molecules.

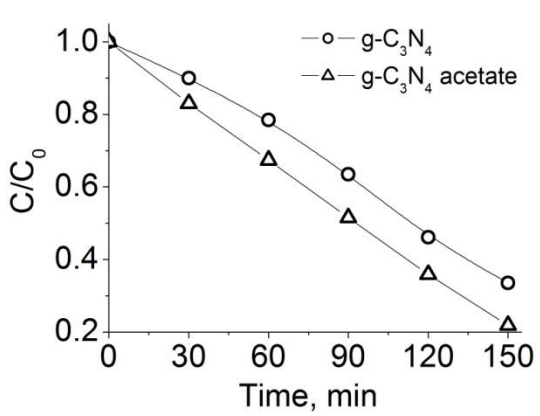

a

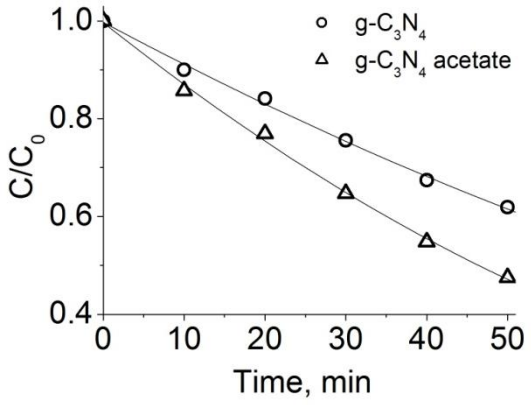

b

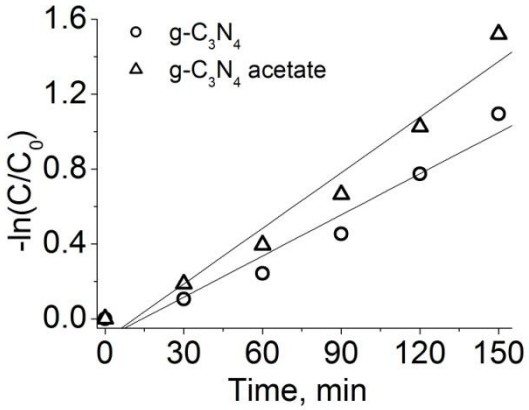

Sample	k', min^{-1}	R^2
g-C_3N_4	0.006	0.955
g-C_3N_4 acetate	0.008	0.964

c

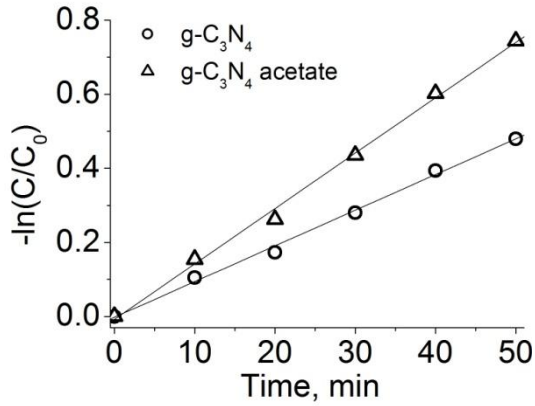

Sample	k', min^{-1}	R^2
g-C_3N_4	0.010	0.996
g-C_3N_4 acetate	0.015	0.999

d

Fig. 5. (a, b) Kinetic curves and (c, d) pseudo-first order linear plots of Rhodamin B degradation on g-C_3N_4 and g-C_3N_4-acetate depends UV-radiation wavelengths: (a) 320-400 and (b) 240-320 nm.

For "hard" UV irradiation (type B), a two times increase in the rate of Rhodamine B catalytic degradation was observed for g-C_3N_4 (k' of 0.010 min^{-1}) and g-C_3N_4-acetate (k' of 0.016 min^{-1}) samples (Fig. 5d). Thus, the dye degradation degree on g-C_3N_4 and g-C_3N_4-acetate samples within 50 min reached of 0.40 and 0.55, respectively (Fig. 5b).

Conclusions

The samples of graphitic carbon nitride were synthesized by method of melamine thermal condensation. It was found that the use of pre-treated melamine with acetic acid leaded to a slight shift in the peaks of thermal transformations and practically did not effect on the g-C_3N_4 crystal and chemical structure. Significant differences in the porous structure of the samples were revealed, which lead to the formation of a larger-pore g-C_3N_4-acetate sample ($D_{des.BJH}$ of 27.9 nm), characterized by a lower specific surface (A_{BET} of 11.5 m^2/g) compared to g-C_3N_4 (A_{BET} of 17.2 m^2/g).

Firstly, the influence of precursor nature on the catalytic activity of g-C_3N_4 in the reaction of Rhodamine B photocatalytic degradation was studied. It was shown that g-C_3N_4-acetate sample characterized by higher activity due to the large-porous structure and a more efficient dye molecules adsorption: the degree of Rhodamin B degradation reached 0.7 (at 150 min) and 0.55 (at 50 min) under “soft” (type A) and “hard” (type B) UV irradiation, respectively. It was found that for “hard” (type B) UV irradiation, the rate of Rhodamine B degradation increased in two times and the apparent rate constant (k') was 0.010 min^{-1} (g-C_3N_4) and 0.016 min^{-1} (g-C_3N_4-acetate). This allows considering the g-C_3N_4-acetate sample as a promising photocatalyst for wastewater treatment from organic pollutants.

Conflict of interests

The authors declare that they have no conflict of interest.

Acknowledgment

The authors are grateful to Evgeniy Krut’ko, researcher of the laboratory of photochemistry and electrochemistry of IGIC NAS Belarus for his help in performing the photocatalytic experiment.

References

Chen, D.; Cheng, Y.; Zhou, N.; Chen, P.; Wang, Y.; Li, K.; Huo, Sh.; Cheng, P.; Peng, P.; Zhang, R.; Wang, L.; Liu, H.; Liu, Y.; Ruan, R. "Photocatalytic degradation of organic pollutants using TiO_2-based photocatalysts: A review". *J. Cleaner Prod.*, 2020, 268, article ID 121725. https://doi.org/10.1016/j.jclepro.2020.121725.

Dong, G.; Zhang, Y.; Pan, Q.; Qiu, J. " A fantastic graphitic carbon nitride (g-C_3N_4) material: Electronic structure, photocatalytic and photoelectronic properties". *J. Photochem. Photobiol. C: Photochem. Rev.*, 2014, 20, 33-50. http://dx.doi.org/10.1016/j.jphotochemrev.2014.04.002.

He, F.; Wang, Zh.; Li, Y.; Peng, Sh.; Liu, B. "The nonmetal modulation of composition and morphology of g-C_3N_4-based photocatalysts". *Appl. Catal., B*, 2020, 269, article ID 118828. https://doi.org/10.1016/j.apcatb.2020.118828.

Ivanets, A.; Prozorovich, V.; Roshchina, M.; Grigoraviciute-Puroniene, I.; Zarkov, A.; Kareiva, A.; Wang, Zh.; Srivastava, V.; Sillanpää, M. "Heterogeneous Fenton oxidation using magnesium ferrite nanoparticles for Ibuprofen removal from wastewater: optimization and kinetics studies". *J. Nanomater.*, 2020 (2020), article ID 8159628, https://doi.org/10.1155/2020/8159628.

Lu, F.; Astruc, D. "Nanocatalysts and other nanomaterials for water remediation from organic pollutants". *Coord. Chem. Rev.*, 2020, 408, article ID 213180, https://doi.org/10.1016/j.ccr.2020.213180.

Thomas, N.; Dionysiou, D. D.; Pillai, S. C. "Heterogeneous Fenton catalysts: A review of recent advances". *J. Hazard. Mater.* , 2021, 404 (Part B), article ID 124082, https://doi.org/10.1016/j.jhazmat.2020.124082.

Thommes, M.; Kaneko, K.; Neimark, A. V.; Olivier, J. P.; Rodriguez-Reinoso, F.; Rouquerol, J.; Sing, S. W. "Physisorption of gases, with special reference to the evaluation of surface area and pore size distribution (IUPAC Technical Report)". *Pure Appl. Chem.*, 2015, 87(9-10), 1051-1069. https://doi.org/10.1515/pac-2014-1117.

Valeikiene, L.; Roshchina, M.; Grigoraviciute-Puroniene, I.; Prozorovich, V.; Zarkov, A.; Ivanets, A.; Kareiva, A. "On the reconstruction peculiarities of sol-gel derived $Mg_{2-x}M_x/Al_1$ (M = Ca, Sr, Ba) layered double hydroxides". *Crystals*, 2020, 10(6), 470-488. https://doi.org/10.3390/cryst10060470.

Wang, W.; Niu, Q.; Zeng, G.; Zhang, Ch.; Huang, D.; Shao, B.; Zhou, Ch.; Yang, Y.; Liu, Y.; Guo, H.; Xiong, W.; Lei, L.; Liu, Sh.; Yi, H.; Chen, Sh.; Tang, X. "1D porous tubular g-C_3N_4 capture black phosphorus quantum dots as 1D/0D metal-free photocatalysts for oxytetracycline hydrochloride degradation and hexavalent chromium reduction". *Appl. Catal., B*, 2020, 273, article ID 119051. https://doi.org/10.1016/j.apcatb.2020.119051.

Wu, M.; Yan, J.-M.; Zhang, X.-W.; Zhao, M. "Synthesis of g-C_3N_4 with heating acetic acid treated melamine and its photocatalytic activity for hydrogen evolution". *Appl. Surf. Sci.*, 2015, 354(Part A), 196-200. https://doi.org/10.1016/j.apsusc.2015.01.132.

Yang, Y.; Li, X.; Zhou, Ch.; Xiong, W.; Zeng, G.; Huang, D.; Zhang, Ch.; Wang, W.; Song, B.; Tang, X.; Li, X.; Guo, H. "Recent advances in application of graphitic carbon nitride-based catalysts for degrading organic contaminants in water through advanced oxidation processes beyond

photocatalysis: A critical review". *Water Res.*, 2020, 184, article ID 116200. https://doi.org/10.1016/j.watres.2020.116200.

Zhang, J.; Chen, X.; Takanabe, K.; Maeda, K.; Domen, K.; Epping, J. D.; Fu, X.; Antonietti, M.; Wang, X. "Synthesis of a carbon nitride structure for visible-light catalysis by copolymerization". *Angew. Chem. Int. Ed.*, 2010, 49, 441-444. https://doi.org/10.1002/anie.200903886.

Zhang, J.; Zhang, M.; Zhang, G.; Wang, X. "Synthesis of carbon nitride semiconductors in sulfur flux for water photoredox catalysis". *ACS Catal.*, 2012, 2(6), 940-948. https://doi.org/10.1021/cs300167b.

Zhang, T. "Heterogeneous Catalytic Process for Wastewater Treatment". Advanced Oxidation Processes. Applications, Trends, and Prospects (Bustillo-Lecompte, C. (Ed.)). Intech Open Limited, London. 2020, 1-30. https://doi.org/10.5772/intechopen.90393.

Zhao, G.; Zou, J.; Chen, X.; Yu, J.; Jiao, F. "Layered double hydroxides materials for photo (electro-) catalytic applications". *Chem. Eng. J.*, 2020, 397, article ID 125407. https://doi.org/10.1016/j.cej.2020.125407.

Zhu, D.; Zhou, Q. "Action and mechanism of semiconductor photocatalysis on degradation of organic pollutants in water treatment: A review". *Environ. Nanotechnol. Monit. Manage.*, 2019, 12, article ID 100255. https://doi.org/10.1016/j.enmm.2019.100255.

Received 11.10.2020
Revised 25.11.2020
Accepted 28.11.2020

ВПЛИВ КИСЛОТНОЇ ОБРОБКИ МЕЛАМІНУ НА ФІЗИКО-ХІМІЧНІ ВЛАСТИВОСТІ ТА КАТАЛІТИЧНУ АКТИВНІСТЬ G-C_3N_4

[1]А. Іванець, [1]В. Прозорович*

[1]Інститут загальної та неорганічної хімії Національної академії наук Білорусі, Мінськ, 220072, Білорусь.

[*]Автор для листування: ivanets@igic.bas-net.by

Реферат

Гетерогенні фотокаталізатори широко використовуються для очищення стічних та природних вод від органічних забруднювачів. У цій роботі фотокаталізатори на основі g-C_3N_4 були синтезовані термічною конденсацією меламіну. Вплив попередньої обробки

меламіну оцтовою кислотою на фізико-хімічні властивості g-C_3N_4 вивчали за допомогою диференціального термогравіметричного аналізу (DTA-TG), дифракції рентгенівських променів (XRD), спектроскопії FT-IR, скануючої електронної мікроскопії (SEM) та низьких - температура адсорбції-десорбції азоту. Каталітичну активність синтезованих фотокаталізаторів оцінювали під час окислювальної деградації родаміну B у водному розчині при «м'якому» (тип A) та «жорсткому» (тип B) УФ-опроміненні.

Ключові слова: g-C_3N_4; Синтез; Прогресивні окислювальні процеси; Фотокаталізатор; Родамін B; Очищення стічних вод